Room-Temperature Reversible Spin Hall Effect

T. Kimura,[1,2] Y. Otani,[1,2] T. Sato,[1] S. Takahashi,[3,4] and S. Maekawa[3,4]

[1]*Institute for Solid State Physics, University of Tokyo 5-1-5 Kashiwanoha, Kashiwa, Chiba 277-8581, Japan*

[2]*RIKEN FRS, 2-1 Hirosawa, Wako, Saitama 351-0198, Japan**

[3]*Institute for Materials Research, Tohoku University, Sendai, Miyagi 980-8577, Japan*

[4]*CREST, JST, Honcho 4-1-8, Kawaguchi, Saitama, 332-0012, Japan*

(Received 13 September 2006; published 12 April 2007)

Reversible spin Hall effect comprising the direct and inverse spin Hall effects was electrically detected at room temperature. A platinum wire with a strong spin-orbit interaction is used not only as a spin current absorber but also as a spin-current source in the specially designed lateral structure. The obtained spin Hall conductivities are 2.4×10^4 $(\Omega\mathrm{m})^{-1}$ at room temperature, 10^4 times larger than the previously reported values of semiconductor systems. Spin Hall conductivities obtained from both the direct and inverse spin Hall effects are experimentally confirmed to be the same, demonstrating the Onsager reciprocal relations between spin and charge currents.

DOI: 10.1103/PhysRevLett.98.156601 PACS numbers: 72.25.Ba, 72.25.Mk, 75.70.Cn, 75.75.+a

The basic science for electronic devices aiming at manipulating the spin degree of freedom is spintronics, which provides a possible means to realize advantageous functionalities for spin based recording and information processing. For such functions, the usage of spin current, a flow of spin angular momentum, is indispensable. Thus establishing techniques for efficient generation and manipulation of spin currents is a key for further advancement of spintronic devices. There is a novel phenomenon where the spin-orbit interaction converts a charge current into a spin current and vice versa [1–3], known as the ''direct'' and ''inverse'' spin Hall effects (SHEs).

The SHE was first predicted in 1971 by D'yakonov and Perel [1], followed by the phenomenological theory with impurity scattering developed by Hirsch [2], and extended to the diffusive transport regime by Zhang [3]. Recently, the SHE has attracted considerable interest because of the potential for generation and manipulation of spin currents in nonmagnets without external magnetic fields. Kato *et al.* reported the first experimental observation of the direct SHE induced spin accumulation via the magneto-optical Kerr effect in GaAs semiconductor systems [4]. Following this measurement, measurements suggesting the intrinsic SHE in a 2 DEG system were performed through the detection of photoluminescence from a LED heterostructure [5]. Moreover, generation of the spin and charge current due to SHE have been observed in GaAs at 80 K using two-color optical coherence control techniques [6]. More recently, the room-temperature SHE has been observed in Cl-doped ZnSe [7]. However, the obtained SH conductivity is as small as 0.5 $(\Omega\mathrm{m})^{-1}$ because of the small spin-orbit interaction. For semiconductor systems reported so far, the optical detection technique is commonly utilized to measure the SHE because their spin diffusion lengths are much larger than the spot size of the laser beam of the order of 1 μm. Therefore, this technique cannot be applied for the system with nanometer-scale spin diffusion lengths due to strong spin-orbit interaction. It should be noted here that the electrical detection of the SHE in semiconductor systems has never been demonstrated up to now. Two kinds of extrinsic [1–3] and intrinsic [8,9] mechanisms for the SHE have been so far proposed to explain the experimental results in semiconductor systems [4,5,10], but the detailed origin of the observed phenomena is still under discussion.

In diffusive normal metals, the SHE is known to be induced by the spin-orbit scattering originating as an extrinsic effect due to impurities or defects [3,11–14]. Since the optical detection technique is limited for semiconductor systems, the electrical detection is the only way to access the SHE in diffusive metals. The unpolarized charge current flowing in a nonmagnet generates the transverse spin current, and results in the spin accumulation along the side edge of the nonmagnet. Inversely, the spin current flowing in a nonmagnet induces the transverse charge current, and causes the charge accumulation (inverse SHE) [14,15]. Very recently, the electrical observation of the charge accumulation due to the inverse SHE has been made by using a nonlocal spin injection in a lateral ferromagnetic-nonmagnetic metal structure [16]. However, the observation was performed only at low temperatures possibly because of a small spin-orbit interaction of aluminum. To induce a large measurable inverse SHE even at room temperature, a large spin-orbit scattering is required. Platinum is known to exhibit a large spin-orbit interaction because of the large atomic number with respect to nonmagnetic impurities or defects [17]. However, the conventional lateral structure [16,18] with nonlocal spin injection is not applicable to detect the SHE because of an extremely short spin diffusion length of about 10 nm [17]. There is an experimental report of the charge accumulation due to the inverse SHE in the Pt strip using a spin pumping technique [19]. However, the large sample size makes it difficult to evaluate the important parameters related to the SHE such as spin-current induced and charge-current induced SH conductivities. Unfortunately,

in metallic systems, only the inverse SHE has been observed by the above groups. Therefore, there still remains an urgent task to measure electrically both the direct and inverse SHE for quantitative analyses of the SH conductivities.

Here we report the first clear electrical detection of the spin and charge accumulations due to the direct and inverse SHEs both at room temperature and 77 K induced in the Pt wire with a nanoscale spin diffusion length using a specially developed electrical detection technique combined with the spin-current absorption. This technique enables us to detect the spin-Hall signal generated over the spin diffusion length of a few nanometers in the system with strong spin-orbit interaction. We also show that the spin-current-induced and the charge-current-induced SH conductivities are the same, corresponding to the experimental demonstration of the Onsager reciprocal relations between the direct and the inverse SHEs.

Our device for the present SHE experiment consists of lateral ferromagnetic-nonmagnetic metallic junctions as shown in Fig. 1(a). The device consists of a large permalloy (Py) pad 30 nm in thickness, a Cu cross 100 nm in width and 80 nm in thickness, and a Pt wire 80 nm in width and 4 nm in thickness. The size of the junction between the Py injector and Cu wire, is chosen to be 100 nm $\times$ 100 nm to induce a large spin accumulation in the Cu wire. The distance from the center of the injector to the center of the Pt wire is 400 nm. The resistivities of the Py, Cu, and Pt are 15.4×10^{-8} Ωm, 2.1×10^{-8} Ωm, and 15.6×10^{-8} Ωm at RT.

When the charge current is injected from a ferromagnetic Py pad into a nonmagnetic Cu cross and is drained from one of the top and bottom arms [see inset of Fig. 2(b)], the accumulated spins at the junction induce the diffusive flow of the spin-current along the Cu wire as can be understood from the electrochemical potential map in Fig. 1(b). When the distance between the Py/Cu and Cu/Pt junctions d is shorter than the spin diffusion length of about 500 nm [20], the spin current should be absorbed into the Pt wire from the Cu cross. According to previous experiments [21], the magnitudes of the spin current and spin accumulation can be calculated by taking into account the spin resistance, defined as $R_S = \lambda/[\sigma S(1 - P^2)]$ with the spin diffusion length λ, the spin polarization P, the conductivity σ, and the effective cross-sectional area S for the spin current [14,21]. The spin current in the spin-accumulated material is thus preferably absorbed into the additionally connected material with small spin resistance. Here the spin resistance of Pt wire is an order of magnitude smaller than that of Cu wire. Therefore, the induced spin current in the Cu cross can be directed into the Pt wire as shown in Fig. 1(c).

The injected spin current into the Pt wire vanishes immediately in the vicinity of the Pt/Cu junction because of the short spin diffusion length of the Pt. Hence, the spin current flows almost perpendicular to the junction plane as in Fig. 1(c) [21,22]. The charge current $\boldsymbol{I}_C$ is generated in

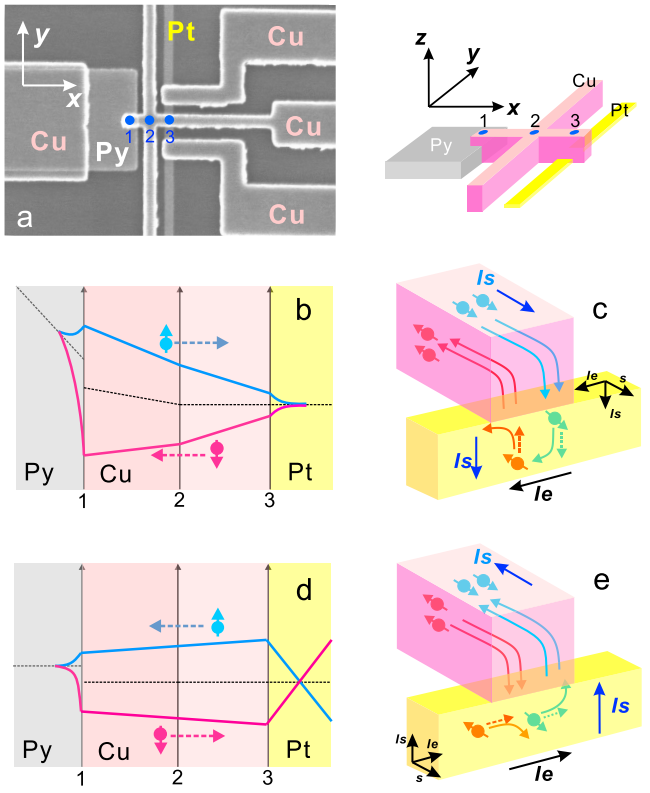

FIG. 1 (color online). (a) Scanning electron microscope (SEM) image of the fabricated spin Hall device together with a schematic illustration of the fabricated device. (b) Schematic spin dependent electrochemical potential map indicating spin accumulation in Cu and Pt induced by the spin injection from the Py pad. Dashed line represents the equilibrium position. (c) Schematic illustration of the charge accumulation process in the Pt wire, where $\boldsymbol{I}_S$ and $\boldsymbol{I}_e$ denote injected pure spin current and induced charge current, respectively. (d) Spin dependent electrochemical potential map for the charge to spin-current conversion and (e) corresponding schematic illustration.

the Pt wire via the inverse SHE when the spin current $\boldsymbol{I}_S$ enters the Pt wire. The direction of the current $\boldsymbol{I}_C$ is given by the vector product $\boldsymbol{s} \times \boldsymbol{I}_S$, where $\boldsymbol{s}$ is the spin direction, yielding the flow of charge current normal to both $\boldsymbol{I}_S$ and $\boldsymbol{s}$. As shown in Figs. 1(b) and 1(c), the up- and down-spin electrons flow opposite to each other as the flow of the electron is determined by the gradient of electrochemical potential. Such flows of up- and down-spins could induce the transverse voltage due to the spin-orbit interaction. Thus, when the spin currents polarized along the x axis are injected into the Pt wire, the charge accumulation along the y axis is induced in the Pt wire. It should be remarked here that the inverse transformation from $\boldsymbol{I}_C$ to $\boldsymbol{I}_S$ is also expected when the configuration of injector and detector probes is reversed as illustrated in Figs. 1(d) and 1(e).

In order to observe the charge accumulation due to the inverse SHE, we first measure the Hall voltage V_C induced in the Pt wire by means of the nonlocal spin injection. The spin-polarized charge current is injected from the Py pad into the Cu cross. The magnetic field is applied along the x

axis to maximize the charge accumulation in the Pt wire. As shown in Figs. 2(a) and 2(b), the clear change in $\Delta V_C/I$ appears both at RT and 77 K. The $\Delta V_C/I$ curves show hysteresis, assuring that the charge accumulation is induced by the spin current from the Py injector. The magnitude of ΔR_{SHE}, defined as the overall change of $\Delta V_C/I$, is increased up to 160 mΩ at 77 K. The observed change in signal does not depend on the choice of the Cu arm and the similar results were observed in other two devices, assuring good reproducibility. In order to verify the effect to be the SHE, the current was injected from the top Cu arm and drained from the bottom. This leads to no spin accumulation in the Cu wire. As a result, no voltage change along the Pt wire was observed as a function of the applied field. This indicates that the observed signal changes are purely caused by the spin injection from the Py pad since no other spurious effects can explain the observed results. Furthermore, we have measured the signal as a function of the distance between the injector Py and the absorber Pt. The signal monotonically decreases with increasing the distance and is well described by Eq. (1) discussed later with the room-temperature spin diffusion length 500 nm for the Cu wire [20]. These also prove that the amount of the spin accumulation in the Cu wire determines the intensity of the spin current absorbed into the Pt wire which is actually converted to the charge current [23]. One should notice that in this device configuration the charge accumulation can be induced by the in-plane component of the Py magnetization. This is a great advantage because the influence of the demagnetizing field can be avoided. Furthermore, unlike previous metallic devices, the magnetization direction of the spin injector Py can be controlled at will by small in-plane magnetic fields below a few hundreds Oe.

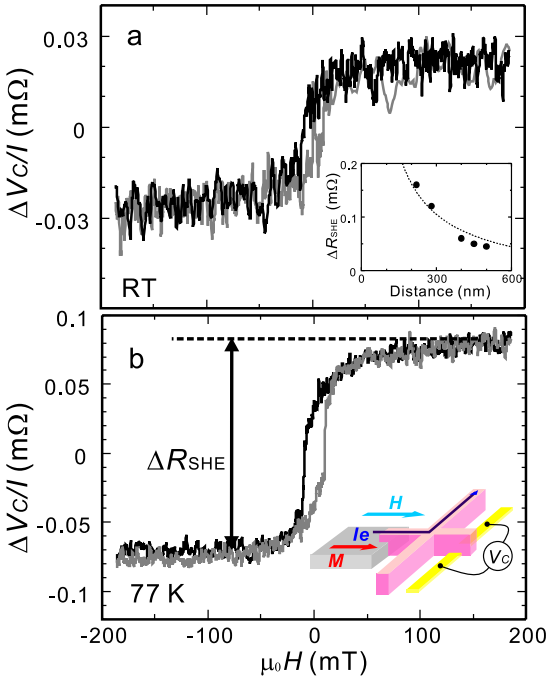

FIG. 2 (color online). The change in Hall resistance $\Delta V_C/I$ due to the inverse spin Hall effect (SHE) (a) at room temperature and (b) at 77 K. The inset of (a) shows the dependence of ΔR_{SHE} on the distance between the injector and the Pt wire at room temperature. The dotted line is a fitted curve using Eq. 2 with $\lambda_{\mathrm{Cu}} = 500$ nm. Here, the different device geometry is utilized for $d = 220$ and 280 nm devices[23]. The inset of (b) shows the probe configuration for the measurement. The measurements are performed by using a current-bias lock-in technique with the excitation current of 300 μA.

To understand the relation between the direction of the injected spins $\boldsymbol{s}$ and the induced charge accumulation, the angular dependence of $\Delta V_C/I$ is measured as a function of the in-plane field $\boldsymbol{H}$ along the tilting angle ϕ from the x axis. The induced ΔR_{SHE} decreases with transverse magnetic component [Figs. 3(a) and 3(b)], and vanishes when the magnetization is aligned with the y axis [Fig. 3(c)]. From the relation $\boldsymbol{I}_{\mathrm{C}} \propto \boldsymbol{s} \times \boldsymbol{I}_{\mathrm{S}}$, the angular dependence of the ΔR_{SHE} is expected to vary with $\cos\phi$. Figure 3(d) shows clear $\cos\phi$ variations of ΔR_{SHE} both at RT and 77 K in good agreement with the prediction.

Finally, the transformation from $\boldsymbol{I}_{\mathrm{C}}$ to $\boldsymbol{I}_{\mathrm{S}}$, which is the direct SHE, is examined using the probe configuration in the inset of Fig. 4(b). It should be noted that in the above described experiment, the Pt wire is used as a spin-current absorber, but the Pt wire now acts as a spin-current source. for the application of spintronics without using a ferromagnet. Figures 4(a) and 4(b) show the field dependences of the induced spin accumulation signal $\Delta V_S/I$ in the Pt wire measured at RT and 77 K. $\Delta V_S/I$ varies similarly to $\Delta V_C/I$ in Figs. 2(a) and 2(b) and more importantly the overall resistance change ΔR_S is exactly the same as ΔR_{SHE}. The angular dependence of the direct SHE also shows the same cosine variation as in the inverse SHE.

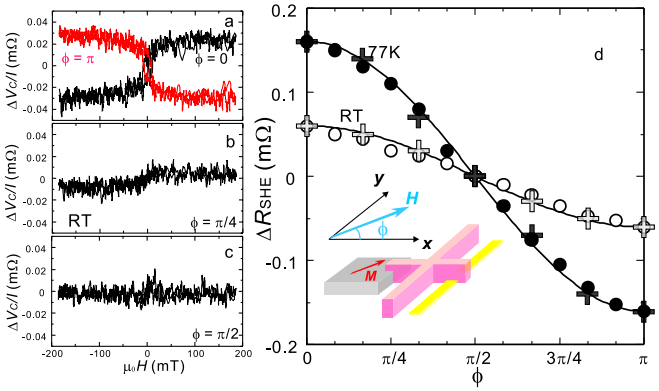

FIG. 3 (color online). Hall resistance change due to the inverse SHE at room temperature for various directions [(a) $\phi = 0$, (b) $\phi = \pi/4$ and (c) $\phi = \pi$] of the external magnetic field. (d) Overall Hall resistance change ΔR_{SHE} as a function of the direction of the magnetic field. The solid lines are $\cos\phi$ curves best fitted to the results. Crosses represent the data points determined from the direct SHE measurements, indicating both inverse and direct SHEs exhibit the same angular dependence.

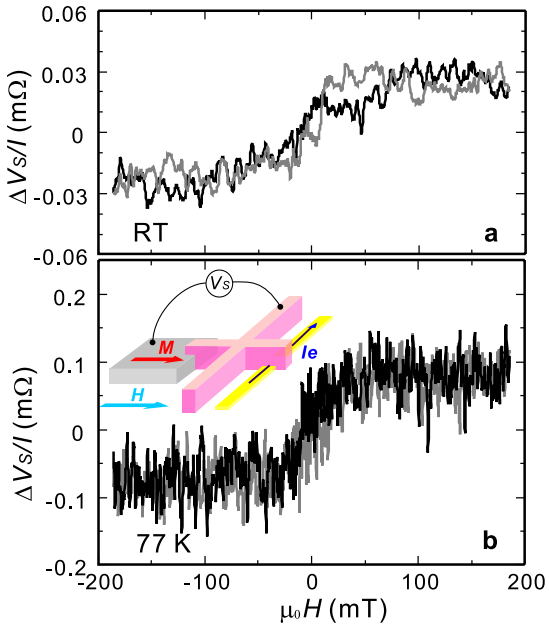

FIG. 4 (color online). Spin accumulation signal $\Delta V_S/I$ generated by SHE at room temperature and 77 K. Field dependences of the signal are similar to those in Figs. 2(a) and 2(b). The exciting current for the lock-in measurements is limited below 60 μA to prevent Joule heating of the thin Pt wire 4 nm in thickness. To obtain a reasonable S/N ratio in the signal for the room-temperature measurement, 30 curves are averaged. Because of the insufficient S/N ratio, the hysteresis behaviors cannot be seen clearly.

These results demonstrate that both the spin to charge and the charge to spin-current transformations are reversible, corresponding to the Onsager reciprocal relations, $\sigma_{\mathrm{SHE}} = \sigma'_{\mathrm{SHE}}$, where σ_{SHE} and σ'_{SHE} are, respectively, the spin-current-induced SH conductivity and the charge-current-induced SH conductivity [8]. The SH conductivity of the Pt wire is here evaluated as follows: In the experiments of inverse SHE, by assuming that both the spin resistances $R_{S\mathrm{Py}}$ of Py and $R_{S\mathrm{Pt}}$ of Pt are much smaller than $R_{S\mathrm{Cu}}$ of Cu[14,21,22], the injected spin current I_{Si} into the Pt wire is approximated by $I_{\mathrm{Si}} \approx P_{\mathrm{Py}} I_C (R_{S\mathrm{Py}}/R_{S\mathrm{Cu}}) \times [\sinh(d/\lambda_{\mathrm{Cu}})]^{-1}$, where λ_{Cu}, P_{Py} and I_C are the spin diffusion length of Cu, the spin polarization of Py, and the injected charge current. The SH conductivity σ_{SHE} can be given by the following equation [3,12,16]:

$$\sigma_{\mathrm{SHE}} \approx \left(\frac{w\sigma_{\mathrm{Pt}}^2}{P_{\mathrm{Py}}}\right)\left(\frac{R_{S\mathrm{Cu}}}{R_{S\mathrm{Py}}}\right)\sinh\left(\frac{d}{\lambda_{\mathrm{Cu}}}\right)\Delta R_{\mathrm{SHE}}, \qquad (1)$$

where w is the width of the Pt wire (80 nm in the present study). By using $P_{\mathrm{Py}} = 0.2$, $\lambda_{\mathrm{Py\ at\ RT}} = 3$ nm, $\lambda_{\mathrm{Cu\ at\ RT}} = 500$ nm and we obtain the value of σ_{SHE} as 2.4×10^4 $(\Omega\mathrm{m})^{-1}$ at RT 10^4 times larger than the values reported in semiconductor systems [4,7] and 10 times larger than that for Al obtained in a previous experiment [16]. The ratio of the SH conductivity to the electrical conductivity $\alpha_{\mathrm{SHE}} = \sigma_{\mathrm{SHE}}/\sigma$ for Pt is deduced to be 3.7×10^{-1}, which is also the largest value reported so far, as expected from the larger atomic number of Pt. The dimensionless spin-orbit parameter η_0 can also be calculated to be 0.74 from the relation $\eta_0 \approx (k_F l)\alpha_{\mathrm{SHE}}$ with the Fermi wave vector $k_F \approx 1 \times 10^{10}$ m^{-1} and the mean free path $l \approx 20$ nm for Pt [17]. This is quantitatively in good agreement with the value of 0.80 separately calculated using the equation $(3\sqrt{3}\pi/2)(R_K/k_F^2)(\sigma/\lambda)$ with the quantum resistance R_K [14]. This result opens up a new possibility to use normal metals with high spin-orbit coupling as spin-current sources operating at room temperature for the future spintronic applications.

*Electronic address: kimura@issp.u-tokyo.ac.jp

[1] M. I. D'yakonov and V. I. Perel, Phys. Lett. **35**, 459 (1971).
[2] J. E. Hirsch, Phys. Rev. Lett. **83**, 1834 (1999).
[3] S. Zhang, Phys. Rev. Lett. **85**, 393 (2000).
[4] Y. K. Kato, R. S. Myers, A. C. Gossard, and D. D. Awschalom, Science **306**, 1910 (2004).
[5] J. Wunderlich, B. Kaestner, J. Sinova, and T. Jungwirth, Phys. Rev. Lett. **94**, 047204 (2005).
[6] H. Zhao, E. J. Loren, H. M. van Driel, and A. L. Smirl, Phys. Rev. Lett. **96**, 246601 (2006).
[7] N. P. Stern *et al.*, Phys. Rev. Lett. **97**, 126603 (2006).
[8] J. Sinova *et al.*, Phys. Rev. Lett. **92**, 126603 (2004).
[9] S. Murakami, N. Nagaosa, and S. C. Zhang, Science **301**, 1348 (2003).
[10] V. Sih *et al.*, Nature Phys. **1**, 31 (2005).
[11] R. V. Shchelushkin and A. Brataas, Phys. Rev. B **71**, 045123 (2005).
[12] R. V. Shchelushkin and A. Brataas, Phys. Rev. B **72**, 073110 (2005).
[13] S. Takahashi and S. Maekawa, Phys. Rev. Lett. **88**, 116601 (2002).
[14] S. Takahashi, H. Imamura, and S. Maekawa, in *Concepts in Spin Electronics*, edited by S. Maekawa (Oxford University, Oxford, 2006).
[15] E. M. Hankiewicz *et al.*, Phys. Rev. B **72**, 155305 (2005).
[16] S. O. Valenzuela and M. Tinkham, Nature (London) **442**, 176 (2006).
[17] H. Kurt *et al.*, Appl. Phys. Lett. **81**, 4787 (2002).
[18] F. J. Jedema, A. T. Filip, and B. J. van Wees, Nature (London) **410**, 345 (2001).
[19] E. Saitoh, M. Ueda, H. Miyajima, and G. Tatara, Appl. Phys. Lett. **88**, 182509 (2006).
[20] T. Kimura, J. Hamrle, and Y. Otani, Phys. Rev. B **72**, 014461 (2005).
[21] T. Kimura, Y. Otani, and J. Hamrle, Phys. Rev. B **73**, 132405 (2006).
[22] S. Takahashi and S. Maekawa, Phys. Rev. B **67**, 052409 (2003).
[23] L. Vila, T. Kimura, and Y. Otani (unpublished).